Hindawi
Shock and Vibration
Volume 2019, Article ID 6078342, 10 pages
https://doi.org/10.1155/2019/6078342

Research Article

Impact of Moisture Content on the Dynamic Failure Energy Dissipation Characteristics of Sandstone

Aihong Lu,[1,2] **Shanchao Hu**,[1,2] **Ming Li**,[2] **Tianzhu Duan**,[3] **Bing Li**,[4] **and Xiya Chang**[1,2]

[1]*School of Mechanics & Civil Engineering, China University of Mining and Technology, Xuzhou, Jiangsu 221008, China*
[2]*State Key Laboratory for Geomechanics and Deep Underground Engineering, China University of Mining and Technology, Xuzhou, Jiangsu 221008, China*
[3]*China Coal Technology Engineering Group Chongqing Research Institute, Chongqing 400039, China*
[4]*School of Civil Engineering, Xuzhou Institute of Technology, Xuzhou 221002, China*

Correspondence should be addressed to Shanchao Hu; kdhushanchao@163.com

Received 10 November 2018; Revised 20 January 2019; Accepted 5 March 2019; Published 27 March 2019

Academic Editor: Yuri S. Karinski

Rockburst frequently occurs in deep underground engineering, which poses a threat to safety and causes economic losses. Water injection into surrounding rock masses is an effective method for preventing rockburst, and the moisture content of rocks is significant for assessing the probability of rockburst. However, the majority of studies focus on the relationship between the macromechanical properties of rock masses under static loads and the moisture content of rock masses and seldom explore the impact of moisture variation (under dynamic loads) on the mechanical properties and energy dissipation. In this paper, the mechanical properties and energy dissipation of sandstone with different moisture contents have been experimentally investigated by the split Hopkinson pressure bar (SHPB) test. The test results indicate that the peak strength, dynamic elastic modulus, and unloading elastic modulus of sandstone in dry conditions are considerably larger than those in moisture conditions, and the three parameters linearly decrease as the moisture content increases from 0% to 2.58%. The distribution law of sandstone fragments with different moisture contents has been investigated by sieving test fragments with different grain sizes of grading sieves. The results show that the percentage of large grain size fragments incrementally decreases, and the percentage of small grain size fragments incrementally increases with moisture contents from 0% to 2.58%. When the moisture content ranges from 2.01%~2.58%, the fractal dimension linearly increases, which indicates that the higher the moisture content is, the larger the dimension of the broken sandstone is. The calculation results for energy indicate that the sandstone energy attains the peak value with 0% moisture content. When the moisture content ranges from 2.01%~2.58%, the reflected energy increases, and the transmitted energy and dissipated energy linearly decrease. In addition, the surface energy of the sandstone with different moisture contents has been investigated by converting fragments into spheres with the corresponding size. The results indicate that the smallest surface area of sandstone is obtained in dry conditions, but its surface energy in dry conditions is larger than that in moisture conditions. When the moisture ranges from 0% to 2.58%, due to 3% illite and 2% chlorite clay minerals reacting with different proportions of moisture, the surface areas of sandstone fragments linearly increase and the surface energy of sandstone linearly decreases.

1. Introduction

Water has an important impact on deformation and failure of rock masses, and the variation in the moisture content of rock masses may cause a significant change in the internal energy and induce major geological disasters; e.g., landslides usually occur after heavy rains [1]. All geotechnical engineering, including tunnel excavation, subway construction, and deep coal mining, involves the dynamic failure of rocks with different moisture contents under explosion loads or impact loads. Therefore, considering the moisture content as a prominent factor in this dynamic failure problem, the analysis of the moisture content, mechanical properties, energy dissipation, fractal dimension of fragments, and surface energy of rock masses under impact loads is important to deep coal mining and underground geotechnical engineering.

Rocks are brittle materials with heterogeneous composite structures; their plastic deformation energy is substantially smaller than their surface energy. Thus, the failure of the surrounding rock masses during deep coal mining primarily depends on whether the surface energy of rock masses is balanced with the external input energy. Due to the action of a water environment, the physical and mechanical properties of rock masses are significantly degraded, including the elastic modulus, friction coefficient [2, 3], surface free energy [4, 5], and strength [6, 7]. The variation in the physical properties further changes the original brittleness of rock masses. Kim and Changani [1] conducted static, quasistatic, and dynamic loading tests on red and buff sandstone in two conditions: dry state and saturated water state. According to the test results, the strength of red sandstone and Buff sandstone in the saturated state was approximately 20% lower than that in the dry state. Liu et al. [8] conducted a uniaxial compression creep test on a slate sample with different moisture contents using an Instron electrohydraulic servo. The test results indicated a linear negative correlation between the elastic modulus and the saturation and a negative exponential correlation between the viscoelastic modulus and the viscosity coefficient with saturation, as well as an increase in the deformation with an increase in the saturation. Peschel [9] noted that the compressive strength of igneous rocks and metamorphic rocks was reduced by approximately 3–15% due to water saturation. Tianbin et al. [10] conducted a conventional triaxial compression test under the confirming pressures of 20, 30, and 40 MPa with 5 different moisture contents ($\omega = 0$, $\omega = 0.2\omega_s$, $\omega = 0.5\omega_s$, $\omega = 0.7\omega_s$, and $\omega = \omega_s$, where ω_s is the saturated mass moisture content) using MTS815. The test results indicated that the growth rate of the total absorbed energy of rock masses and their total energy decreased as the moisture content increased, and the elastic energy decreased in the energy storage stage as the moisture content increased. Wasantha and Ranjith [11] conducted a triaxial test on Hawkesbury sandstone in both the dry state and saturated state under the confining pressures of 4, 10, 18, and 25 MPa. According to the test results, the angle of the shear failure surface decreased as the confining pressure increased, and the angle decreased from 55° to 45° in the dry state and from 50° to 40° in the saturated state. However, the angle in the dry state was distinctly larger than that in the saturated water state under the same pressure. Wong et al. [12] investigated the impact of water on the strength and stiffness of rock masses and established the relationship among the compressive strength, tensile strength, and elastic modulus. Zhang et al. [13] discovered that the compressive strength of siltstone decreased and the damage variable increased as the moisture content increased in the uniaxial compression process. A series of results indicate that moisture has a substantial impact on the physical and mechanical properties of rocks.

With the need for more deep coal mining projects and the development of test technology, some scholars have investigated the dynamic compressive mechanical properties of rock masses under the water environment in recent years. Zhou et al. [14] conducted a dynamic impact compression test of the sandstone with a 100 S^{-1} (±5) strain rate in the dry state and a moisture content of 1.0%, 2.0%, and 3.5% using the SHPB system. The test results indicated a negative exponential reduction of the peak stress with an increase in the moisture content. In addition, they conducted a dynamic impact tension test on the sandstone within the same strain rate range with this moisture content. The test results indicated that the peak strength decreased as the moisture content increased. Kim and Martins de Oliveira [15] tested red sandstone and Buff sandstone in both the dry state and the saturated water state within the porosity range of 5.5%–22.5% using the SHPB test. The test results indicated that the maximum stress and maximum strain rate of sandstone in the dry state were larger than those in the saturated water state, and the variation law of the maximum strain contradicted that of the maximum stress and maximum strain rate. According to the research conducted by Pu et al. [16–18] on the dynamic mechanical properties of rocks with different moisture contents, the root cause of the rock strength reduction due to moisture is the mechanical effect and chemical action of moisture on rocks in terms of materialogy [19–24].

According to the current studies, researchers generally focus on the relationship between the macromechanical properties of rock masses under static loads and the moisture content variation and seldom explore the impact of moisture variation (under dynamic loads) on the mechanical properties and energy dissipation. Therefore, in this paper, the relationship between the mechanical properties, energy dissipation, and the moisture content has been investigated by conducting the SHPB impact compression test on the sandstone with different moisture contents (0, 2.01%, 2.23%, 2.40%, 2.49%, 2.53%, and 2.58%). In addition, the law of impact of moisture content on the surface energy of sandstone has been explored based on the dissipated energy and different grain sizes of fragments.

2. Sample Preparation and Method

2.1. Sample Preparation. The sample for the test was collected from a quarry in Xuzhou and processed in a cylinder with a diameter of 50 mm and height of 100 mm. First, a Φ50 mm rock sample was collected from sandstone using a coring machine. Second, a rock sample with a height of approximately 50 mm was cut using a cutting machine. Lastly, the rock sample with a diameter equal to its height was polished to ensure the flatness and parallelism of the two end faces. A basic mechanical property test was conducted on the well-processed sandstone sample. The X-ray diffraction semiquantitative phase analysis showed that the red sandstone mineral composition contained 78% quartz, 13% feldspar (10% plagioclase and potassium feldspar 3%), 3% calcite, 3% illite, 2% chlorite, and 1% hematite. The physical and mechanical parameters are listed in Table 1.

Table 1: The physical and mechanical parameters of sandstone.

E (GPa)	σ_c (MPa)	V (m·s^{-1})	P (kg·m^{-3})	σ_t (MPa)	μ
7.98	20.91	3431	2410	3.37	0.13

Note. E is the elastic modulus, σ_c is the compression strength, V is the sound velocity, P is the density, σ_t is the tensile strength, and μ is Poisson's ratio.

2.2. Sandstone Samples with Different Moisture Contents. After measurement of the moisture content of the site-collected sandstone, the moisture content of the sandstone was controlled during the test to ensure consistency with the site-measured moisture content of sandstone.

(1) To ensure the dryness of the sample, it was placed in a dryer; after drying the sample at 105°C for 24 h, it was weighed. The sample was repeatedly dried until the difference between the two weighed masses was less than 0.01 g. The sandstone was completely dried, and the sample mass was recorded.

(2) The dried sample was placed in a humidifier with 12%, 15%, 18%, 21%, 24%, and 27% humidity values for 24 hours, and the pattern was taken out, and the moisture on the surface of the pattern was blotted with absorbent paper and then weighed and recorded. The moisture content of sandstone can be calculated using the following equation [25]:

$$\omega = \frac{m_a - m_d}{m_d} \times 100\%, \tag{1}$$

where m_a is the mass after wetting; m_d is the mass after drying; and ω is the moisture content of sandstone.

By calculation with equation (1), the moisture contents of 2.01%, 2.23%, 2.40%, 2.49%, 2.53%, and 2.58% were obtained for the sandstone samples in the dry state (0.00%).

2.3. Test Equipment and Method. The split Hopkinson rod experimental technique is the most important and reliable experimental method for studying the mechanical properties of materials under medium and high strain rates and is an important part of the experimental techniques of explosion and impact dynamics.

The SHPB test system (shown in Figure 1) was utilized for the test. The test system (Figure 2) includes five parts: loading drive system, pressure bar system, energy absorption system, signal acquisition system, and signal processing system. The SHPB test system is based on a one-dimensional stress wave assumption and uniform stress propagation assumption. To ensure one-dimensional propagation of stress waves and eliminate the dispersion effect during propagation, a pulse shaper was added at the contact end of the incident bar and impact bar. The pulse shaper is a Φ22 mm rubber sheet with a thickness of 3 mm.

The test process is as follows: first, open the equipment in the signal acquisition system and signal processing system; second, apply a certain quantity of Vaseline to the end of the sandstone sample and place it in the middle of the incident bar and transmission bar; and at last, adjust the air pressure in the emitting chamber and open the control valve at 0.24 MPa air pressure driven by high pressure gas, and then the impact bar impacts the incident bar to complete impact.

Figure 1: Split Hopkinson pressure bar testing system.

Figure 3 is the original waveform in the oscilloscope, in which the yellow curve is the strain signal collected by the strain gauge on the incident rod, the first peak is the incident wave, the second peak is the reflected wave, and the green is the incident wave transmitted through the sandstone pattern. The projected wave is collected by the strain gauge on the transmission rod.

Figure 4 shows the SHPB test waveform of sandstone. As shown in the figure, the incident wave is approximately a sine wave, and its rising edge time is approximately 100 μs, which conforms to the stress uniformity assumption in the SHPB test. The superposed form of the incident wave with the reflected wave is approximately equal to the transmitted waveform, which conforms to the one-dimensional propagation assumption in the SHPB test. The test waveform reflects that the test satisfies the stress uniformity assumption and the one-dimensional stress wave hypothesis. According to the Hopkinson pressure bar test requirements, the performance of these test data reflects the performance of sandstone.

According to the one-dimensional stress wave propagation assumption, the three-wave method equation processed with the SHPB test technical data can be obtained using the following equation [26]:

$$\begin{aligned} \dot{\varepsilon} &= \frac{C_S}{I}\left[\varepsilon_i(t) - \varepsilon_r(t) - \varepsilon_t(t)\right], \\ \varepsilon &= \frac{C_S}{I}\int_0^t \left[\varepsilon_i(t) - \varepsilon_r(t) - \varepsilon_t(t)\right]dt, \\ \sigma &= \frac{A_S}{2A_0}E_0\left[\varepsilon_i(t) - \varepsilon_r(t) - \varepsilon_t(t)\right], \end{aligned} \tag{2}$$

where $\dot{\varepsilon}$ is the average strain rate of the sample; C_S is the stress wave velocity in the bar; $\varepsilon_i(t)$, $\varepsilon_r(t)$, and $\varepsilon_t(t)$ denote the strain signal of the incident wave, reflected wave, and transmitted wave, respectively; I is the original length of the

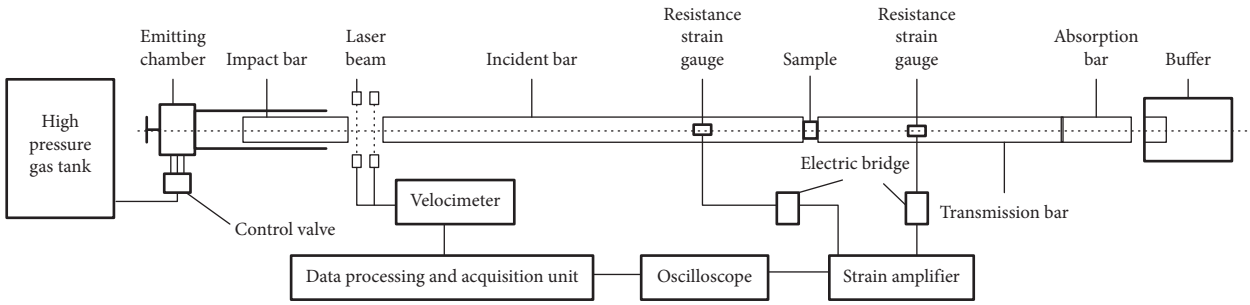

Figure 2: Components of SHPB testing system.

Figure 3: Original waveform in the oscilloscope.

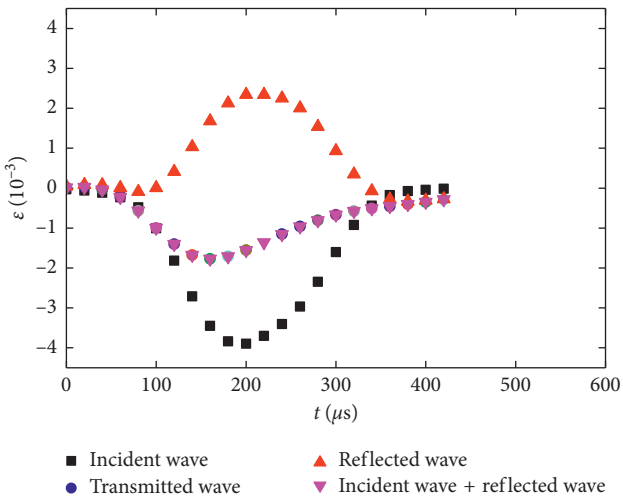

Figure 4: SHPB test waveform of sandstone.

sample; ε is the strain of the sample; σ is the stress of the sample; A_S and A_0 denote the cross section area of the pressure bar and the sample, respectively; and E_0 is the elastic modulus of the bar.

According to the stress uniformity assumption, the stress is equal everywhere in the sample, and equation the following equation can be obtained [26]:

$$\varepsilon_i(t) + \varepsilon_r(t) = \varepsilon_t(t). \tag{3}$$

According to equations (2) and (3), the two-wave method equation for processing SHPB test data can be obtained from

$$\begin{aligned} \dot{\varepsilon}(t) &= -2\frac{C_S}{I}\varepsilon_t(t), \\ \varepsilon(t) &= -2\frac{C_S}{I}\int_0^t \varepsilon_r(t)dt, \\ \sigma(t) &= \frac{A_S}{A_0}E_0\varepsilon_t(t). \end{aligned} \tag{4}$$

3. Impact of Moisture Content on the Mechanical Properties of Sandstone

3.1. Mechanical Properties of Sandstone with Different Moisture Contents. According to equation (4), the stress-strain curve for different moisture contents can be obtained, as shown in Figure 5. The proportion of the compaction stage to the prepeak stage gradually decreases as the moisture content increases. When the moisture content increases, water generates tension inside the original cracks and micropores, which reduces the cohesion among the grains and yields a high rate of shrinkage among the grains. In addition, water fills the defects in the sandstone during compaction; thus, the proportion of the compaction stage decreases as the moisture content increases; the strain range that corresponds with the sample strain-softening process gradually increases as the moisture content increases. After failure of the existing cracks in the sandstone due to an increase in moisture content, additional water infiltrates new cracks and softens them, which enables the new cracks to participate in the test deformation process. The larger the number of postpeak internal defects of the sample is, the larger the resulting softening deformation is. As shown by the unloading failure stage, when the moisture content ranges from 0.00%–2.23%, the unloading curve has an approximately identical slope with the linear elasticity stage. When the moisture content ranges from 2.40%–2.49%, the variation in the unloading failure slope is larger than that of the linear elasticity stage slope. When the moisture content ranges from 2.53%–2.58%, unloading failure decreases along the negative slope.

As shown in Figure 6, the peak stress of sandstone in the moisture state decreases compared with that in the dry state, and the peak stress is linearly reduced in the moisture content variation process. When the moisture content is

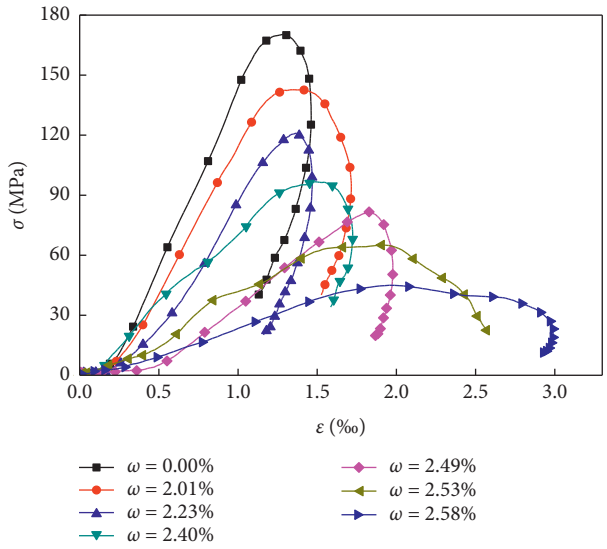

Figure 5: Stress-strain curve of sandstone with different moisture contents.

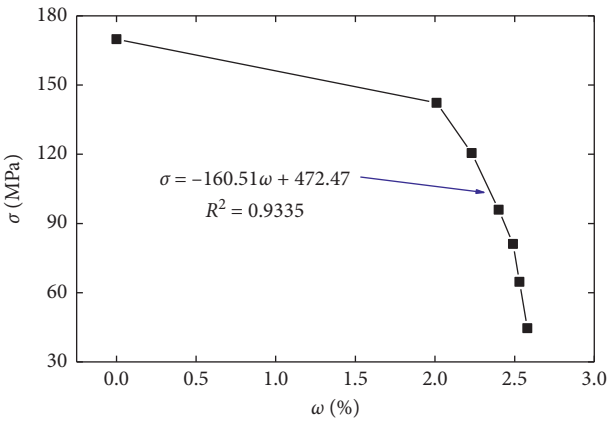

Figure 6: Variation curve of peak stress with moisture content.

increased from 2.01% to 2.58%, the peak stress is reduced from 142.25 MPa to 44.61 MPa and by 68.64% because water enters the sandstone grain clearance to weaken the cohesion among grains and reduce the compressive strength of sandstone. As a kind of soft rock, red sandstone contains about 3% of illite and 2% chlorite clay minerals. It has swelling characteristics under the action of water, which causes the rock particle structure to expand and aggravate the initial damage. In addition, under the action of water chemistry, the particles, the intercalated material, and some mineral components are dissolved so that the microstructure is loose and porous, and the particle connection is weakened [27]. Under the impact load, the initial microcracks in the rock and the loose porous structure after the water absorption and expansion are closed by force, and the strain develops rapidly. Due to the weakening of the rock particle structure, the stress conditions required for the crack initiation of the microcrack are reduced, and the ability of the structure to transmit the load is weakened, which in turn leads to a decrease in the peak stress of the material.

3.2. Failure Characteristics of Sandstone with Different Moisture Contents. Figure 7 shows the morphology of the sandstone after failure at different strain rates. The sandstone samples have been destroyed under different water cuts, but the failure modes and damage degrees differ.

As shown in Figure 6, the effect of water on sandstone particle size is primarily reflected in the following aspects: when the water content is 0.00%, the large-sized fragments in the model are the largest of all large-sized fragments, and the sandstone fragments under water contain water. When the rate is increased, the particle sizes of the large-sized fragments gradually decrease; the number of fragments with smaller particle sizes gradually increases with an increase in the water content, and the water content is 0.00% when the particle size is the lowest.

To better describe the breaking of sandstone with different moisture contents, the test fragments under the action of impact loads are sieved using 0.2 mm, 1 mm, 2.5 mm, 3 mm, 5 mm, 10 mm, 12 mm, 15 mm, 20 mm, and 30 mm standard sieves. Thus, fragments (serial number i: 11–1) of different grades, including 0~0.2 mm, 0.2~1 mm, 1~2.5 mm, 2.5~3 mm, 3~5 mm, 5~10 mm, 10~12 mm, 12~15 mm, 15~20 mm, 20~30 mm, and 30~50 mm, are obtained. Weigh the mass of each grade of fragment with a high sensitivity electronic scale and record the test data.

The percent W_i of the mass of the fragments within each grain size range to the total mass is calculated as follows:

$$W_i = \frac{m_i}{M}, \tag{5}$$

where W_i is the mass percent of fragments with this grain size; m_i is the mass of fragments with this grain size; and M is the total mass of the test block.

Figure 7 provides the percent of the mass of sandstone fragments with different moisture contents to the total mass. As shown in Figure 8, the percent of sandstone fragments with different moisture contents differs; for serial numbers 1 and 2, the percent of sandstone fragments decreases with an increase in the moisture content; for serial numbers 3–11, the percent of sandstone fragments increases with an increase in the moisture content within each grain size range.

3.3. Calculation of Fractal Dimension D. French mathematicians generalized the concept of fractal dimension to fractal geometry. Based on fractal geometry, the broken irregular experiment fragments obtained in the experiment process can be converted to data to accurately describe the breaking law of the test block in the experiment. The fractal dimensions of sandstone fragments are calculated using the mass-equivalent dimension:

$$D = 3 - d, \tag{6}$$

$$d = \frac{\lg\left(M_R/M\right)}{\lg R}, \tag{7}$$

where D is the fractal dimension of the fragments; d is the slope of the straight line plotted in the log-log coordinate;

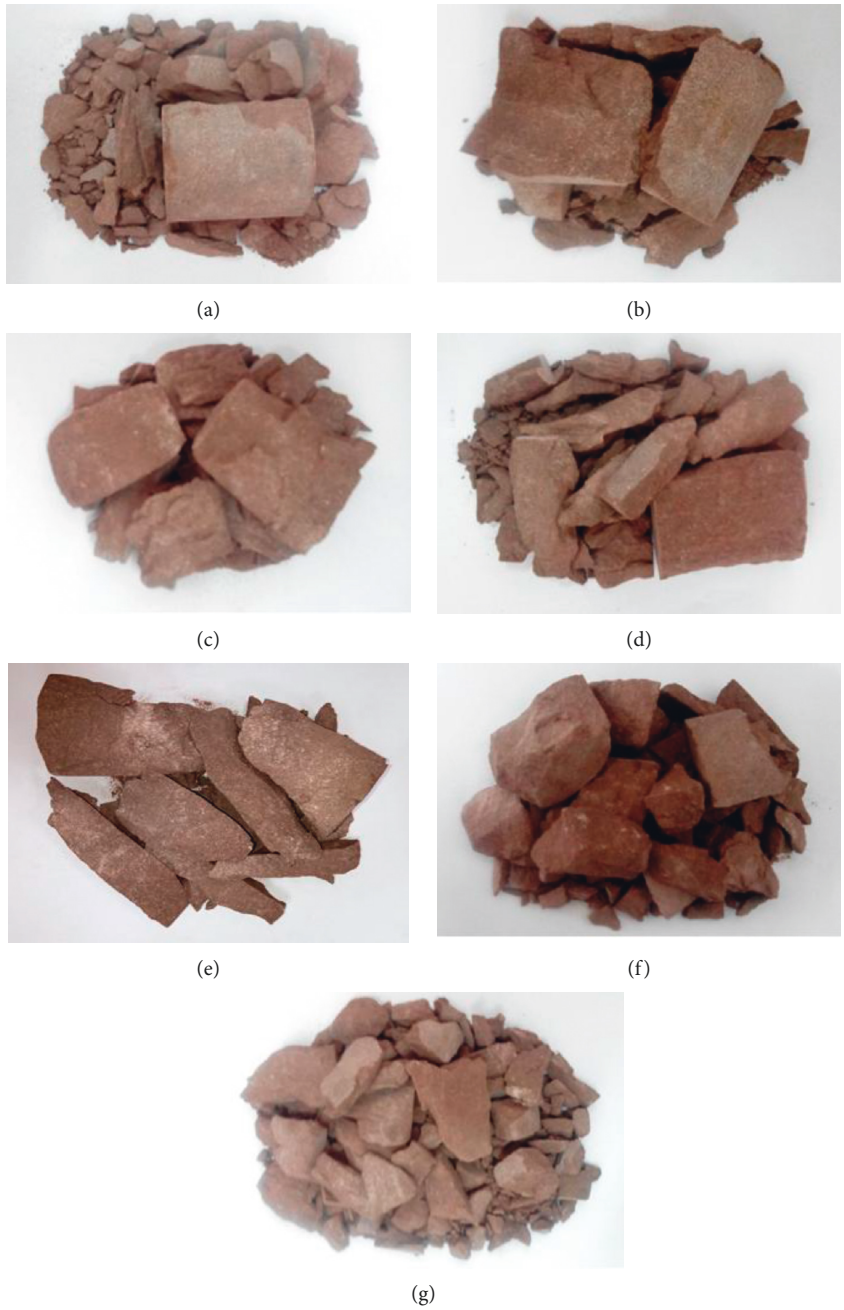

Figure 7: Sandstone failure morphology for different water contents. (a) $\omega = 0.00\%$. (b) $\omega = 2.01\%$. (c) $\omega = 2.23\%$. (d) $\omega = 2.40\%$. (e) $\omega = 2.49\%$. (f) $\omega = 2.53\%$. (g) $\omega = 2.58\%$.

and M_R is the cumulative mass of fragments with a diameter less than R.

The fractal dimension at the mass-equivalent dimension calculated from equations (6) and (7) is shown in Figure 9. The distribution of the fractal dimension of the sandstone fragments with different moisture contents at the mass-equivalent dimension slightly differs; the distribution is centralized in the moisture state, whereas the distribution in the dry state is integrally translated compared with that in the moisture state.

3.4. Relationship of Fractal Dimension D with Moisture Content ω. Figure 10 provides the fractal dimension at the mass-equivalent dimension. As shown in Figure 10, the fractal dimension of the sandstone fragments in the moisture state is generally larger than that in the dry state. When the moisture content ranges from 2.01% to 5.58%, the fractal dimension of the sandstone fragments gradually increases with an increase in the moisture content, and the fractal dimension linearly increases with an increase in the moisture content. This finding indicates that different moisture

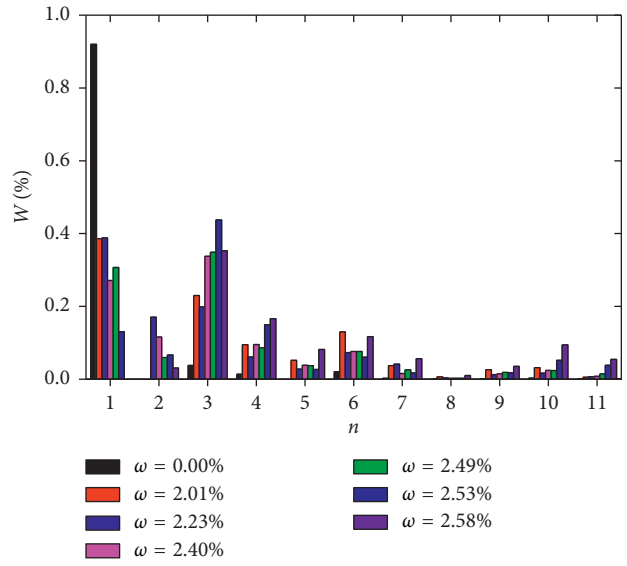

Figure 8: Percent of the mass of fragments with different grain sizes to the total mass of the sample.

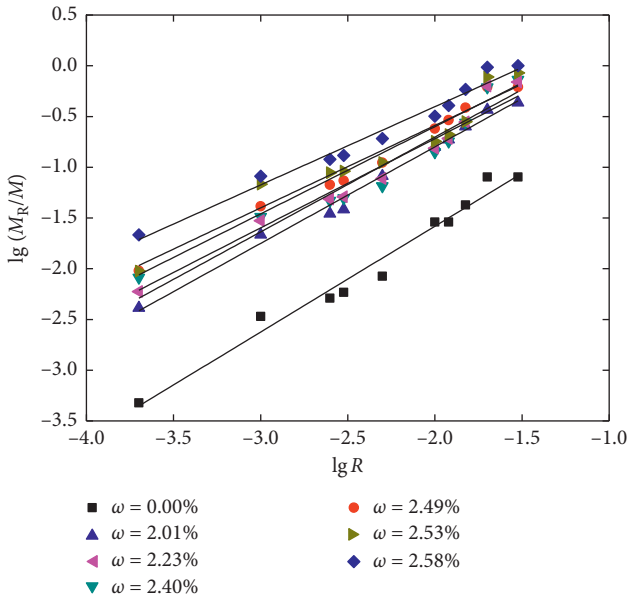

Figure 9: Fractal dimension at mass-equivalent dimension.

contents of sandstone cause different levels of damage to sandstone under the same air pressure condition; the higher the moisture content is, the more substantial the damage to the sandstone is.

4. Energy Variation Law of Sandstone in Moisture State

4.1. Sandstone Energy Calculation Principle. According to the laws of thermodynamics, energy conversion is an essential characteristic of the physical process of substances, and substance damage is a state instability phenomenon driven by energy. Thus, the energy carried by the stress wave is calculated according to

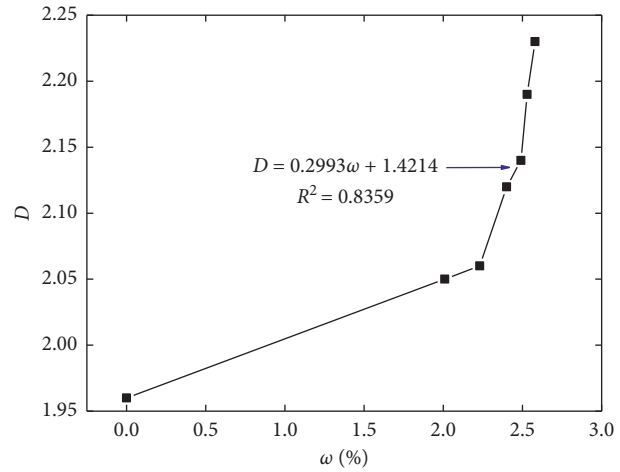

Figure 10: Relationship of fractal dimension D with moisture content ω.

$$W = \frac{AC}{E}\int_0^t \sigma^2(t)dt = ACE\int_0^t \varepsilon^2(t)dt, \tag{8}$$

where A is the cross section area of the incident bar and transmission bar; E is the elastic modulus of the material of the incident bar and transmission bar; and C is the one-dimensional stress wave velocity. In the elastic stage, C is related to the density and elastic module E of the incident bar and can be expressed by

$$C = \sqrt{\frac{E}{\rho}}. \tag{9}$$

According to this equation, the incident energy W_I, reflected energy W_R, and transmitted energy W_T in the SHPB dynamic impact process can be expressed as [28]

$$\begin{aligned} W_I &= ACE\int_0^t \varepsilon_i(t)dt, \\ W_R &= ACE\int_0^t \varepsilon_r(t)dt, \\ W_T &= ACE\int_0^t \varepsilon_t(t)dt, \end{aligned} \tag{10}$$

where W_I, W_R, W_T, and W_L are the incident energy, reflected energy, transmitted energy, and dissipated energy, respectively.

4.2. Energy Dissipation Law of Sandstone with Different Moisture Contents. Figure 11 displays the variation curve of the transmitted energy, reflected energy, and dissipated energy in the system with moisture content. The reflected energy tends to gradually increase, and the transmitted energy and dissipated energy tend to gradually decrease in the test process as the moisture content increases. According to further analyses, as the moisture content increases, the proportion of transmitted energy gradually decreases. When the moisture content increases from 2.01% to 2.23%, the proportion of transmitted energy decreases from 18.96% to

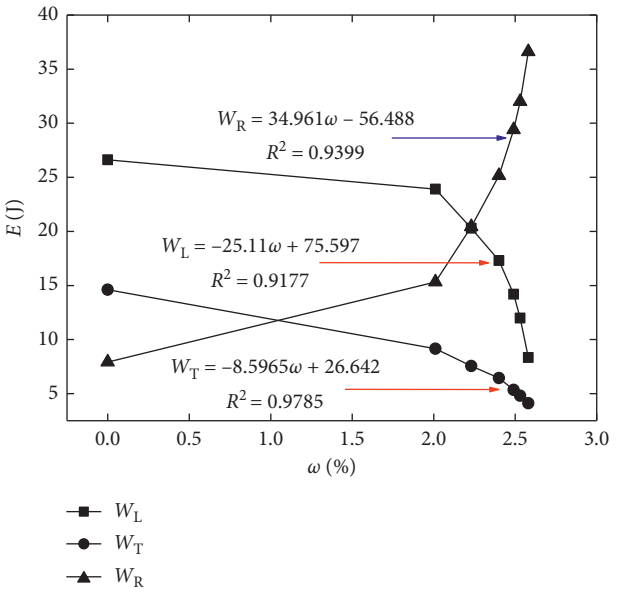

Figure 11: Variation curve of each type of energy in the system with moisture content.

13.43%. When the moisture content increases from 2.23% to 2.49%, the proportion of transmitted energy decreases from 13.43% to 11.26%. When the moisture content increases to 2.58%, the energy dissipation rate decreases to 8.63%. The proportion variation law of reflected energy contradicts that of transmitted energy. The proportion of reflected energy gradually increases, and its variation amplitude gradually increases as the moisture content increases. When the moisture content increases from 2.01% to 2.58%, the proportion of reflected energy increases from 30.82% to 47.03%. The proportion of dissipated energy gradually decreases, and its reduction amplitude gradually increases as the moisture content increases. When the moisture content increases from 2.01% to 2.58%, the proportion of dissipated energy decreases from 50.21% to 44.48%.

The moisture content has a substantial impact on the energy dissipation characteristics in the sandstone failure process: the proportion of reflected energy to the input energy increases with an increase in moisture content. The proportion of transmitted energy and dissipated energy gradually decreases with an increase in the moisture. This finding indicates that the increase in the moisture content of sandstone can effectively reduce the energy utilization rate and the proportion of energy that is wasted due to the transmission in the sandstone failure process.

4.3. Surface Energy Calculation Principle. For brittle material, such as sandstone, dissipated energy primarily exists in the form of surface energy, which causes the separation of fragments. To further probe into the impact of moisture on the dissipated energy and the fractal dimension of sandstone, sandstone fragments are simplified and sieved into the spheres with the corresponding size, as shown in Figure 12 [29].

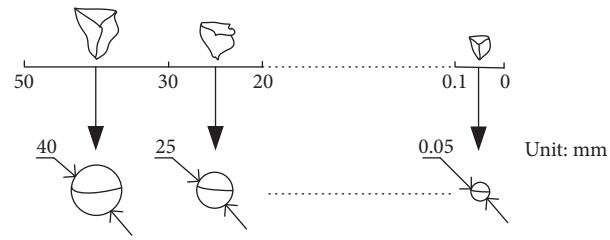

Figure 12: Schematic of converting fragments into spheres.

The number of spheres within the sieving diameter range is calculated from

$$n_i = \frac{m_i}{4\pi\rho r_i^3/3}, \tag{11}$$

where n_i is the number of spheres with size i; m_i is the mass of spheres with size i; and r_i is the radius of spheres at size i.

The surface area of the separated fragments is equal to the sum of all sphere surface areas minus the sum of the original surface areas of the sample. The original surface areas of the sample include the areas of the upper and lower faces and side face of the sample cylinder. Therefore, the sum of the areas of the spheres converted from sandstone fragments with different moisture contents can be expressed by the following equation:

$$S_\omega = \sum_1^{11} 4n_i\pi r_i^2 - 2\pi rh - 2\pi r^2, \tag{12}$$

where r is the radius of the sandstone test block in the impact test and h is the height of the sandstone test block in the impact test.

For the sandstone under the impact effect, the sandstone suffers from the impact effect and is deformed when each part bears the action of external forces. Because external forces act on the sandstone, the faces of sandstone fragments are mutually separated. The sum of the surface energy in the separation process of the faces is the external input energy. Sandstone is a brittle material, and its dissipated energy is primarily manifested as surface energy. Thus, the relation between the surface energy and the dissipated energy is expressed as follows [29]:

$$W_L = S_\omega\lambda_\omega. \tag{13}$$

According to the calculated dissipated energy and the obtained surface area of the fragments, the surface energy of the sandstone fragments on the unit area can be calculated [29]:

$$\lambda_\omega = \frac{W_L}{S_\omega}. \tag{14}$$

4.4. Surface Energy Results Analysis of Sandstone with Different Moisture Contents. According to equations (12) and (14), the law of variation of the surface area and surface energy of sandstone fragments with moisture content can be calculated, as shown in Figure 13. The higher the moisture content is, the larger the equivalent surface area of the

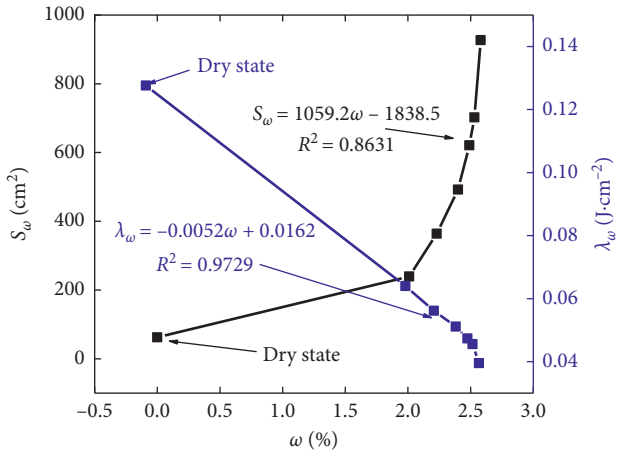

Figure 13: Variation curve of surface area and surface energy with moisture content.

fragments is, as a higher moisture content causes more significant breaking of sandstone and a smaller fragment size. Thus, the equivalent sphere surface area is larger. The surface area of fragments exhibits a normal linear relation with moisture content. According to Figure 13, the largest surface energy of sandstone in the dry state is attained, and the surface energy of sandstone in the moisture state gradually decreases with an increase in moisture content. The surface energy has a linear reduction relation with moisture content.

The dissipated energy and surface energy of sandstone in the dry state attain the largest values, the dissipated energy and surface energy of sandstone in the moisture state linearly decrease with an increase in moisture content, and the surface areas of the fragments increase with an increase in moisture content. The reduction in the surface energy of sandstone is primarily attributed to the softening and erosion effect of the moisture content on sandstone.

Because 3% illite and 2% chlorite clay minerals react with different proportions of moisture, softening and erosion in sandstone is stronger than that in dry sandstone, and the internal cohesion of sandstone is reduced; thus, the water content increased from 2.01% to 2.58%, and the surface energy of sandstone decreased from 0.06396 J·cm^{-2} to 0.03949 J·cm^{-2}, and additional cracks participate in the deformation failure of sandstone when the incident energy is almost identical to generate a large number of failure surfaces.

5. Conclusions

In this paper, the results of the mechanical properties and energy dissipation of sandstone with different moisture contents have been obtained by conducting dynamic impact tests on the sandstone with different moisture contents at 0.24 MPa air pressure using the SHPB test. The following conclusions have been obtained from the analysis of these results:

(1) Moisture content has a substantial impact on the stress-strain curve of sandstone. The proportion of the compaction stage to the prepeak stage gradually decreases with an increase in moisture content. As the moisture content increases, the strain range that corresponds with the strain-softening process gradually increases and the unloading slope gradually decreases from large to small and from positive to negative. The peak strength linearly decreases with moisture.

(2) According to the sieving analysis results of fragments, the proportion of fragments with a large grain size gradually decreases and that of fragments with small grain sizes gradually increases with an increase in moisture content. In addition, the fractal dimension linearly increases with an increase in the moisture content, which indicates the gradually increase in the damage to sandstone.

(3) Reflected energy differs from transmitted energy and dissipated energy in the variation law with an increase in the moisture content. Reflected energy in the moisture state is slightly higher than that in the dry state. As the moisture content increases, the total amount and increasing speed of the reflected energy gradually increase. The variation law of transmitted energy and dissipated energy contradicts that of the reflected energy, and the total amount of transmitted energy and dissipated energy gradually decreases with an increase in the moisture content.

(4) According to the analysis results of the conversion of fragments into spheres with the corresponding size, the cumulative surface area of spheres with different sizes gradually increases with an increase in the moisture content; the surface energy of sandstone has a linear relation with the moisture content; and as the moisture content of sandstone increases, the surface energy of sandstone gradually decreases and has a linear reduction relation with the moisture content.

Data Availability

The data used to support the findings of this study are available from the corresponding author upon request.

Conflicts of Interest

The authors declare that they have no conflicts of interest.

Acknowledgments

The authors gratefully acknowledge the financial support of this study provided by the Research Program of Xuzhou Institute of Technology (XKY2016228) and Basic Research on Prevention and Control of Geological Disasters and Environmental Protection under High-Intensity Coal Mining in West China (2013CB227900).

References

[1] E. Kim and H. Changani, "Effect of water saturation and loading rate on the mechanical properties of red and buff sandstones," *International Journal of Rock Mechanics and Mining Sciences*, vol. 88, pp. 23–28, 2016.

[2] J. Byerlee, "Friction of rocks," *Pure and Applied Geophysics PAGEOPH*, vol. 116, no. 4-5, pp. 615–626, 1978.

[3] C. A. Morrow, D. E. Moore, and D. A. Lockner, "The effect of mineral bond strength and adsorbed water on fault gouge frictional strength," *Geophysical Research Letters*, vol. 27, no. 6, pp. 815–818, 2000.

[4] B. K. Atkinson, "Subcritical crack growth in geological materials," *Journal of Geophysical Research: Solid Earth*, vol. 89, no. B6, pp. 4077–4114, 1984.

[5] T. A. Michalske and S. W. Freiman, "A molecular interpretation of stress corrosion in silica," *Nature*, vol. 295, no. 5849, pp. 511-512, 1982.

[6] M. S. Paterson, *Experimental Rock Deformation: The Brittle Field*, Springer-Verlag, Berlin, Germany, 1978.

[7] M. S. Paterson and T.-F. Wong, *Experimental Rock Deformation—The Brittle Field*, Springer-Verlag, Berlin, Germany, 2005.

[8] X. Liu, C. Yang, and J. Yu, "The influence of moisture content on the time-dependent characteristics of rock material and its application to the construction of a tunnel portal," *Advances in Materials Science and Engineering*, vol. 2015, Article ID 725162, 7 pages, 2015.

[9] A. Peschel, "Zur ermittlung und bewertung von festigkeitseigenschaften bei natursteinen," *Zeitschrift für Angewandte Geologie*, vol. 20, no. 3, pp. 118–128, 1974.

[10] L. I. Tianbin, Z. Chen, G. Chen et al., "An experimental study of energy mechanism of sandstone with different moisture contents," *Rock and Soil Mechanics*, vol. 36, no. 2, pp. 229–236, 2015.

[11] P. L. P. Wasantha and P. G. Ranjith, "Water-weakening behavior of Hawkesbury sandstone in brittle regime," *Engineering Geology*, vol. 178, no. 8, pp. 91–101, 2014.

[12] L. N. Y. Wong, V. Maruvanchery, and G. Liu, "Water effects on rock strength and stiffness degradation," *Acta Geotechnica*, vol. 11, no. 4, pp. 713–737, 2016.

[13] Y.-B. Zhang, L. Cui-ping, P. Liang et al., "Experimental study on the impact of water on rock compressive strength," in *Proceedings of the International Forum on Energy, Environment Science and Materials (IFEESM)*, vol. 40, pp. 58–62, Shenzhen, China, September 2015.

[14] Z. Zhou, X. Cai, W. Cao, and C. Xiong, "Influence of water content on mechanical properties of rock in both saturation and drying processes," *Rock Mechanics and Rock Engeering*, vol. 49, no. 8, pp. 10–24, 2016.

[15] E. Kim and D. B. Martins de Oliveira, "The effects of water saturation on dynamic mechanical properties in red and buff sandstones having different porosities studied with split Hopkinson pressure bar (SHPB)," *Applied Mechanics and Materials*, vol. 752-753, pp. 784–789, 2015.

[16] Y. Pu and M. A. Qinyong, "Split Hopkinson pressure bar tests on sandstone in coalmine under cyclic wetting and drying," *Rock and Soil Mechanics*, vol. 34, no. 9, pp. 2557–2562, 2013.

[17] Y. Pu and M. A. Ruiqiu, "Analysis of energy absorption by rocks with different moisture contents in SHPB tests," *Acta Armamentarii*, vol. 34, no. 1, pp. 328–332, 2013.

[18] Y. Pu and M. A. Ruiqiu, "Split Hopkinson pressure bar tests and analysis of coalmine sandstone with various moisture contents," *Chinese Journal of Rock Mechanics and Engineering*, vol. 34, no. 1, pp. 2888–2893, 2015.

[19] E. Althaus, A. Friz-Töpfer, C. H. Lempp, and O. Natau, "Effects of water on strength and failure mode of coarse-grained granites at 300°C," *Rock Mechanics and Rock Engineering*, vol. 27, no. 1, pp. 1–21, 1994.

[20] J. D. Natau, D. Petrovski, J. Schuyler, and A. Owens, "The effects of aqueous chemical environments on crack propagation in quartz," *Journal of Geophysical Research: Solid Earth*, vol. 89, no. B6, pp. 4115–4123, 1984.

[21] R. J. Martin and W. B. Durham, "Mechanisms of crack growth in quartz," *Journal of Geophysical Research*, vol. 80, no. 35, pp. 4837–4844, 1975.

[22] H. S. Swolfs, "Chemical effects of pore fluids on rock properties," in *American Association of Petroleum Geologists*, vol. 18, pp. 224–234, CRC Press, Boca Raton, FL, USA, 1972.

[23] Q. Zhang, D. Ma, Y. Wu, and F. Meng, "Coupled thermal–gas–mechanical (TGM) model of tight sandstone gas wells," *Journal of Geophysics and Engineering*, vol. 15, no. 4, pp. 1743–1752, 2018.

[24] Y. Hao, Y. Wu, X. Mao et al., "An elastoplastic softening damage model for hydraulic fracturing in soft coal seams," *Advances in Civil Engineering*, vol. 2018, Article ID 2548217, 12 pages, 2018.

[25] W. Kai, J. Yifeng, and X. U. Chao, "Mechanical properties and stYang haoatistical damage model of coal with different moisture contents under uniaxial compression," *Chinese Journal of Rock Mechanics & Engineering*, vol. 37, no. 5, pp. 1070–1079, 2018.

[26] T.-B. Yin, P. Wang, X.-B. LI, R.-H. Shu, and Z.-Y. Ye, "Effects of thermal treatment on physical and mechanical characteristics of coal rock," *Journal of Central South University*, vol. 23, no. 9, pp. 2336–2345, 2016.

[27] Z. Liu, J. Shao, S. Xie, N. Conil, and W. Zha, "Effects of relative humidity and mineral compositions on creep deformation and failure of a claystone under compression," *International Journal of Rock Mechanics and Mining Sciences*, vol. 103, pp. 68–76, 2018.

[28] P. Qi, L. Xuan, M. A. Qinyong et al., "Broken energy dissipation characteristics of sandstone specimens under impact loads," *Chinese Journal of Rock Mechanics and Engineering*, no. 2, pp. 4197–4203, 2015.

[29] Z. Zhang and F. Gao, *Energy Evolution Mechanism during Rock Deformation and Failure*, China University of Mining and Technology Press, Beijing, China, 2014.